Graphical Abstract (for review)

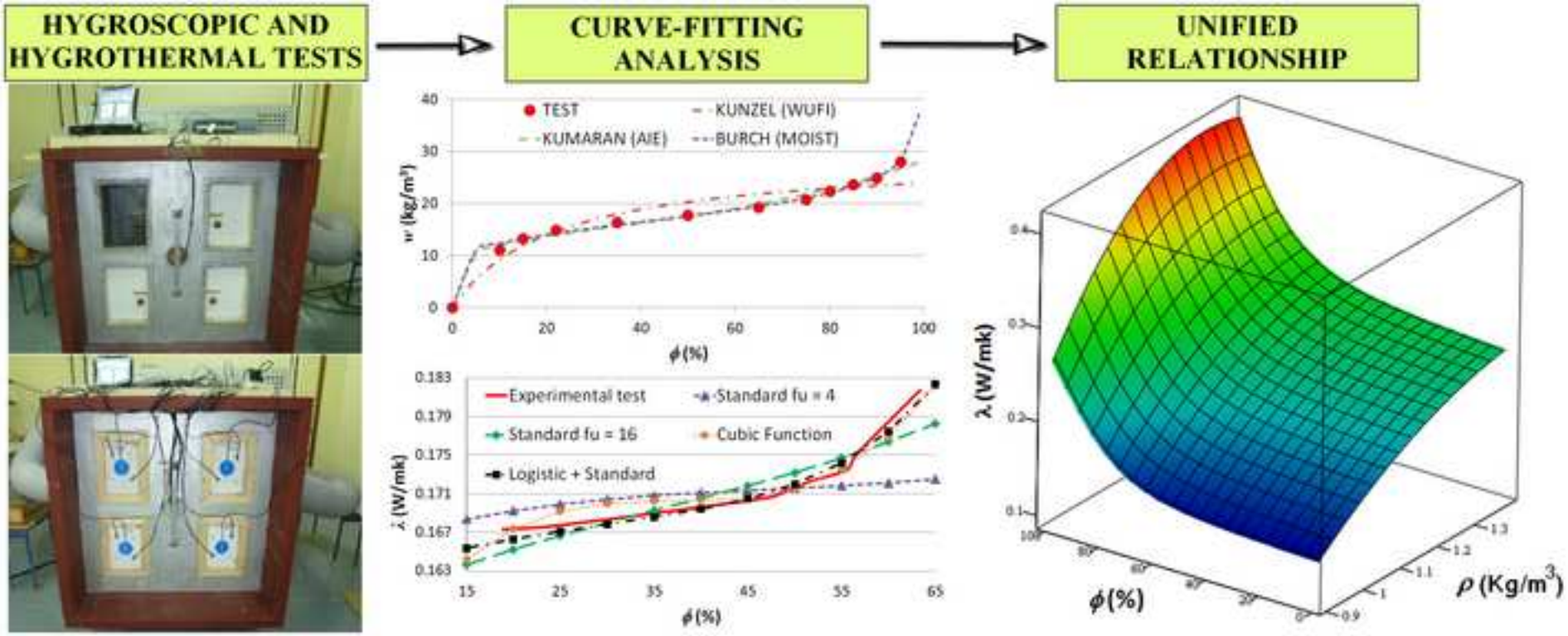

Hygrothermal properties of lightweight concrete: experiments and numerical fitting study

J.J. del Coz Díaz [a,*], F.P. Álvarez Rabanal [a], P.J. García Nieto [b], J. Domínguez Hernández [c], B. Rodríguez Soria [c], J.M. Pérez-Bella [c]

[a]*Department of Construction, University of Oviedo, 33204 Gijon, Spain*
[b]*Department of Mathematics, University of Oviedo, 33007 Oviedo, Spain*
[c]*Department of Construction, University of Zaragoza, 50018 Zaragoza, Spain*

Abstract

This paper presents an experimental research work in order to obtain the main hygrothermal properties of different mixes of lightweight concrete (LWC) produced from expanded clay. Nowadays, the current state of art assumes an exponential relationship between the moisture content and the thermal properties for this kind of building material. The prime novelty of this study is the experimental determination of the actual hygrothermal properties for different LWC mixes with material densities ranging from 900 to 1400 kg/m^3, as well as the least squares best-fitting curves in order to obtain accurate mathematical expressions that permit us to optimize the hygrothermal behaviour of new construction products made up of LWC. In this way, the experimental data set is compared with those for the Standard and a new analytical solution is obtained, giving place to a new analytical solution taking into account the relationship among the heat, moisture and density. Finally, the results and conclusions reached in this work are exposed.

* Corresponding author. Tel.: +34-985-182042; fax: +34-985-182433.
E-mail address: juanjo@construi.uniovi.es (J. J. del Coz Díaz).

Keywords: Lightweight concrete; Heat and moisture transfer; Porous building materials;

Energy savings.

Nomenclature

F_a	conversion factor of aging, dimensionless
F_T	conversion factor of temperature variation, dimensionless
F_m	conversion factor for the moisture content, dimensionless
F_{m_i}	conversion factor for the moisture content of the *i*-th set of conditions
f_u	conversion coefficient of moisture content per unit mass, kg/kg
L	thickness of the specimen across which the temperature difference exists, m
LWA	lightweight aggregate
LWC	lightweight concrete
LWS	lightweight sand
m	specimen mass at equilibrium with a relative humidity, kg
m_0	mass of the dry specimens, kg
n	number of the observed values obtained in the actual tests or '*sample size*'
NWC	normal weight concrete
q	heat flux, or heat flow rate through a surface of unit area perpendicular to the direction of heat flow, W/m^2
r^2	coefficient of determination
R	overall thermal resistance, m^{2}K/W
R_{se}	surface thermal resistance of the specimen in the hot-box test chamber as a function of wind velocity, m^{2}K/W
R_{si}	surface thermal resistance of the specimen in the surrounding area as a function of wind velocity, m^{2}K/W
ΔT	temperature difference between the hot-box and the surrounding area, K
U	heat transmission coefficient or *thermal transmittance*, W/m^{2}K
u	moisture content per unit mass, kg/kg
u_i	moisture content per unit mass of the *i*-th set of conditions, kg/kg
$u_{50\%}$	moisture content per unit mass for $\phi = 50\%$, kg/kg
V	volume of the specimen, m^3
w	moisture content in volume, kg/m^3
Y_i	observed values obtained in the actual tests
$\hat{Y}_i$	modeled values obtained from the fitted curve or *predicted values*
$\overline{Y}$	mean of the observed data

Greek symbols

ϕ	relative humidity (%)
λ	thermal conductivity, W/mK
$\lambda_{50\%}$	thermal conductivity for $\phi = 50\%$, W/mK
ρ	material density, kg/m^3

1. Introduction

In recent years, many researchers have studied the thermal and mechanical properties of different materials used in buildings, such as normal weight concrete (NWC), lightweight concrete (LWC), gypsum, plaster and clay brick [1-8].

LWC has been used in many constructions due to its significant benefits from the structural and thermal points of view. However, more research is necessary to understand the hygrothermal behavior of this porous material. In order to investigate its hygrothermal performance, it is necessary to take into account the material density and its moisture sorption capacity. LWC density typically ranges from 1000 to 1800 kg/m^3 compared with that of 2400 kg/m^3 for NWC. The main advantages of the LWC are the reduction in the dead weight of the structure and good thermal insulation properties due to the cellular structure of the aggregates. The main disadvantage is the porous structure of the aggregate that implies absorption of a significant quantity of the mixing water. This fact has influence in the thermal [7, 8] and mechanical [4] properties of the LWC, causing energy losses and failure cracks, respectively.

Nowadays, the LWC porous material is an important research subject in both heat and moisture transfer points of view due to its attractive characteristics, such as its thermal and acoustic good physical properties, even at high temperatures [8-10]. Some benefits of this research have been applied to the study of the energy efficiency of buildings made up of lightweight concrete products [7, 11]. Furthermore, the basics of the

moisture and heat transfer in porous materials are interesting and current fields of research [12-15] due to their important effects on those steps to avoid the climate change. However, it is possible to state that many recent research studies have often been focused on analytical or numerical investigations instead of experimental measurements [13, 15].

The fundamental references for this research work are those in building physics and focusing on porous building materials and their properties with respect to the heat and moisture transfer. The interested reader is encouraged to consult several recent research works in this field such as advances in simulation tools [10, 11, 13], property measurements [9, 14] and analytical and numerical models [16, 17]. To motivate this discussion, there is a huge interest in the comprehensive study of the heat and moisture transfer between indoor air and hygroscopic building materials due to changes in the indoor humidity since it is clear that this phenomenon may improve air quality and comfort in buildings [18]. In other words, it is necessary to obtain new experimental data to accurately quantify the heat and moisture transfer between hygroscopic building materials and air if the humidity conditions are varied in a cyclical form. Furthermore, these experimental data are also important and a prerequisite for the numerical models that will be used in developing new building products based on LWC.

The main objectives of this research work include: (1) developing a new experimental procedure to obtain the hygrothermal properties of the LWC, (2) studying the thermal properties as a function of the moisture content in LWCs when its density ranges from

900 to 1400 kg/m^3, (3) carrying out different least squares best-fitting curves in order to find an equation that defines the relationship among density, moisture content and thermal conductivity, and (4) proposing a new revised conversion coefficient of thermal conductivity for its use in the ISO 10456:1999 standard [19].

2. Materials and methods

2.1. Material properties

The materials used in this research include expanded clay as then main lightweight aggregate (LWA), lightweight sand (LWS) (see Fig. 1), cement and silica sand. The particle size of the expanded clay ranges from 4 to 12.5 mm for LWA and from 1 to 5 mm for LWS, respectively.

Expanded clay is an artificial lightweight aggregate that is produced firing natural clay in a rotary kiln at the temperature about 1100ºC using a process called "pyroprocessing", which causes the material to expand. The high proportion of semi-closed pores in LWA creates a cellular pore system that supplies to these aggregates their low-particle relative density and good thermal insulated properties.

Fig. 1. Expanded clay aggregates used in this research: LWA (left) and LWS (right).

Table 1

Mix proportions of the LWC samples.

A total of six samples of 0.2 meters width, 0.2 meters long and 0.05 meters thick for different mix proportions (see Table 1) are tested. First of all, the specimens are built in an isolated wood cast in which they are cured during forty eight hours in the laboratory at 23ºC and 48% relative humidity. Next, they were moved from the mould to an oven at 110ºC for 24 hours to achieve the entire dryness of the samples. Then, a 1 mm thick gypsum plaster on both sides is applied, and these specimens are again dried inside the oven for 24 hours more. Finally, it was dried other 72 hours to get an environmental steady state with the laboratory conditions (23ºC and 48% relative humidity). Table 2 shows the densities of the LWC samples tested in this research work.

Table 2

Densities of the LWC determined in this investigation during the manufacturing process.

2.2. Experimental facility

The experimental determination of the LWC hygrothermal properties is carried out using a special testing device based on the Standard's test method for the thermal performance of building assemblies using a *hot-box* apparatus [20, 21]. The special testing device is composed of a climatic chamber connected to an isolated hot-box unit (see Figs. 2 and 3). The thermally isolated hot-box has one cubic meter in volume.

Fig. 2. Scheme of the experimental facility layout.

Fig. 3. Photographs of the climatic chamber (left) and hot-box apparatus (right).

2.3. Hygroscopic test methodology

The Standard ISO 12571:2000 has been used in this research [22]. This Standard is used in this work in order to develop a new test methodology to determine the hygroscopic sorption isotherm of the LWC construction material.

A variant of the air-conditioned room method indicated in the Standard [22] for a climatic test chamber is used in this experimental setup (see Fig. 4). This layout allows that the temperature inside the test chamber remains constant (23 ± 0.5ºC) as well as an increase of the relative humidity ranging from 21% to 95%.

The moisture content of samples is determined by weighing until to obtain a constant mass so that the equilibrium state is reached in each test. The constant mass is achieved when the mass variation between three consecutive weightings, carried out with a time separation of at least 24 hours, becomes less than 0.1% of the total mass of the sample.

The hygroscopic moisture storage is described using the sorption isotherm curves of the material, termed *hygroscopic curves*. These curves establish the relationship between the moisture content for porous media in volume, *V*, or per unit mass, and the relative humidity of air in equilibrium at constant temperature, ϕ, as follows [22]:

$$w(\phi) = \frac{m(\phi) - m_0}{V} \text{ or } u(\phi) = \frac{m(\phi) - m_0}{m_0} = \frac{w(\phi)}{\rho} \quad (1)$$

Fig. 4. Experimental setup (left) and specimens located inside the hot-box test chamber (right) for hygroscopic tests.

2.4. Hygrothermal test methodology

The specific thermal properties determined as a function of the moisture content inside the LWC specimens are: the heat transmission coefficient or *thermal transmittance*, the thermal resistance and the thermal conductivity.

In this way, four samples are placed on a thermal isolated frame using low thermal conductivity foam, located between the test lab environment and the hot-box chamber (see Fig. 5). The hot-box chamber controls the relative humidity and the temperature by means of the climatic generator set so that a dominant horizontal heat flow is achieved.

The temperature, relative humidity and heat flow of the specimen sides are measured to determine the thermal properties of the samples in each test at steady state conditions. For each specimen, five hygrothermal SHT75 capacitive sensors and one HFP01 heat flux sensor are used (see Fig. 5(a-c)). Three hygrothermal sensors are placed on the inner side of the sample (see Fig. 5(d)), and the other two sensors on the external side (see Fig. 5(e)). These sensors are protected with filter caps type SF1 (see Fig. 5(a)) in order to measure the relative humidity and the temperature on the surfaces of the

specimens by means of a data acquisition system (see Fig. 6). Heat flux sensors are placed on the cold side of the samples at room environment (see Fig. 5(e)). Specifically, the hygrothermal conductivity test has taken about 18 hours to complete: 234 hours in total.

Fig. 5. Hygrothermal test setup: (a) a filter cap type SF1, (b) a hygrothermal sensor type SHT75, (c) a thermal flux sensor type HP01, (d) specimens with three sensors type SF1 located on the inner side, (e) specimens with two hygrothermal and one thermal flux sensors on the external side.

Fig. 6. Data acquisition system from temperature and humidity sensors type SHT75.

The main hygrothermal properties are obtained taking into account the following expressions [7, 22, 23]:

$$U = \frac{q}{\Delta T} \tag{2}$$

$$R = \frac{1}{U} + R_{se} + R_{si} \tag{3}$$

$$\lambda = \frac{L}{R} \tag{4}$$

where the value used for the surface thermal resistance of the specimen inside and outside the hot-box test chamber as a function of wind velocity is 0.04 m^2K/W.

2.5. Tests conditions

The test conditions of the experimental tests are:

- Number of samples: six.
- Test environment conditions tested: eleven.
- Volume of each sample: 0.003 m^3.
- Precision weighing balance's accuracy (for hygroscopic tests): ± 0.1 g, 10 kg is the maximum weight allowed.
- Laboratory conditions: 23 ± 1 ºC of temperature and 48 ± 2.5 % of relative humidity.
- Experimental setup: climatic chamber described in subsection 2.3, based on the standards [20-22] using the hot-box apparatus.
- Test site: Moisture Laboratory at High Polytechnic Engineering College of Gijón (University of Oviedo, Principality of Asturias, Northern Spain).

3. Experimental results

The experimental results for the different mixes of LWC studied in this research work are follows as:

- Hygroscopic sorption isotherm (see Eq. 1), used to describe the equilibrium moisture content of the material at a specified constant temperature [22].
- Hygrothermal conductivity or thermal conductivity for different moisture contents (see Eqs. 2, 3 and 4).

3.1. Hygroscopic sorption tests and results

The experimental setup described previously is able to test the hygroscopic properties of several specimens at the same time (see Fig. 4).

The sorption isotherms of the samples checked, the relative humidity as a function of the moisture content expressed in kg/m^3, are shown in Figs. 7, 8 and 9. Table 3 shows the moisture content per unit mass (kg/kg) for the relative humidity points tested.

Fig. 7. Sorption isotherms of the LWC samples type 1.

Fig. 8. Sorption isotherms of the LWC samples type 2.

Fig. 9. Sorption isotherms of the LWC samples type 3.

Table 3

Experimental results of the LWC moisture content per unit mass (kg/kg) for the relative humidity points tested.

From the results obtained in the hygroscopic sorption tests, the following findings are:

- The testing methodology developed in this research work, based on the Standard ISO 12571:2000 [22], is useful to determine the hygroscopic sorption curve of different samples.
- The sorption isotherms of the samples obtained in the tests (see Figs. 7, 8 and 9) and the moisture content per unit mass (see Table 3) show clearly that the moisture absorption is increased in the samples if their density is decreased.

3.2. Hygrothermal conductivity tests

The experimental measurement of the LWC hygrothermal properties is performed by means of the same experimental device (see Fig. 5d-e). Specifically, four specimens are located on a thermal isolated frame at the open front side of the hot-box apparatus.

The temperature differences between the internal and external sides of the specimens located at the hot-box are greater than 15°C in all the tests. This value is recommended by the Standards [20, 21] for these thermal tests. The results obtained for the samples checked are shown in Fig. 10. Additionally, Table 4 shows only the experimental LWC thermal properties for a specific relative humidity equal to 50%.

Fig. 10. Thermal conductivity (λ) versus relative humidity (ϕ) curves for the three different mixtures of LWC.

Table 4

Experimental results of the LWC thermal properties for a relative humidity equal to 50%.

Fig. 11 shows a set of thermal photographs of some specimens checked using the infrared thermographic camera ThermaCAM E300 from FLYR Systems Ltd. It is interesting to observe the evolution of the temperature on the cold side (outer face of the hot-box) for some samples as a function of the relative humidity inside the test chamber. In all cases, the temperature inside the hot-box is equal to 55ºC.

Fig. 11. Thermal photographs of three samples for different relative humidities: 10% (left), 50% (middle) and 80% (right).

Taking into account the results of the tests carried out, the following findings for the hygrothermal properties test of the LWC mixes are:

- The hot-box test chamber provides a stable test environment in order to determine the thermal properties of building elements.
- The laboratory values of the thermal properties belong to the usual range for this LWC material, achieving similar results on specimens of the same type (see Table 4).
- Fig. 11 shows a set of nine thermal imaging photographs corresponding to three samples tested (1A, 2A and 3A) with different moisture contents (10%, 50% and 80%). In all the rows and from left to right, the outside temperature is increased if the moisture content of the sample is also increased. Similarly, in all the

columns and from upper to lower, the outside temperature grows if the sample density is increased.

4. Analytical solution and fitted curves

In order to obtain the most suitable analytical expressions between the thermal properties, moisture content and density of LWC material, it is necessary to calculate the fitted curves from the previous experimental results.

In this sense, the goodness of the fitted curves compared to the observed values is performed using the coefficient of determination as a significant statistic [24, 25]:

$$r^2 = \frac{\sum_{i=1}^{n}\left(Y_i - \hat{Y}_i\right)^2}{\sum_{i=1}^{n}\left(Y_i - \bar{Y}\right)^2} \tag{5}$$

In science and engineering it is often the case that an experiment produces a set of data points $(x_1, y_1),\ldots,(x_n, y_n)$, where the abscissas $\{x_k\}_{k=1}^{n}$ are distinct. One goal of numerical methods is to determine a formula $y = f(x)$ that relates these variables. There are several different possibilities for the type of function that can be used. Usually, a class of allowable formulas is chosen and then the coefficients must be determined. Often there are underlying mathematical models, based on the physical process that will determine the form of the function [25, 26]. This is our case in this research work.

Suppose that we want to fit a nonlinear curve to data points. The original points $(x_1, y_1),...,(x_n, y_n)$ in the *xy*-plane are transformed into the points $(X_1, Y_1),...,(X_n, Y_n)$ in the *XY*-plane. The process that permits to transform a nonlinear fitted curve into a linear fitted curve applying a mathematical transformation in both sides of the equation and introducing a change of variables giving place to a linear relation is called *data linearization*. Finally, the least-squares line is determined minimizing the root-mean-square error, that is to say, solving a linear system known as the *Gaussian normal equations*.

Next, the fitted curves of several theoretical models have been carried out according to the following steps:

1. Transformations for data linearization of the functions for several nonlinear theoretical models. Once the curve has been chosen, a suitable transformation of the variables must be found so that a linear relation is obtained.
2. Finding the best fitted curve with least squares fitting technique using the MATLAB software [26].
3. Refinement of the previous best-fit parameters using a quasi-Newton method. A significant weakness of Newton's method for solving systems of nonlinear equations is that, for each iteration, a Jacobian matrix must be computed and a $n \times n$ linear system solved that involved this matrix. In this work, a generalization of the Secant method to systems of nonlinear equations known as Broyden's method [25] is considered. This method replaces the Jacobian matrix in Newton's method with an approximate matrix for each iteration.

4.1. Hygroscopic fitted curves

In order to obtain the hygroscopic fitted curves, the three most well-known theoretical models to represent the sorption isotherms curves are used:

- The Kunzel model [27, 28]: This model is used by the WUFI moisture transport simulation software, developed at the Fraunhofer-Institut für Bauphysik of Stuttgart. Its mathematical expression is:

$$w(\phi) = w_{\text{lim}} \frac{(b-1)\cdot\phi}{b-\phi} \tag{6}$$

  where w_{lim} and b are the coefficients of the fitted curve.

- The Kumaran model: The catalogue of material properties published in the Annex 14 of the International Energy Agency (IEA) [29, 30], proposes the following function:

$$w(\phi; a, b, c) = \frac{\phi}{a\phi^2 + b\phi + c} \tag{7}$$

  where a, b and c are the coefficients of the fitted curve.

- The Burch model: It was developed by the United States Department of Energy for the MOIST simulation program [31, 32] as follows:

$$w(\phi; A, B) = A\left[\frac{1}{1-\phi} - 1\right]^B \tag{8}$$

  where A and B are the coefficients of the fitted curve.

In order to fit the experimental data of hygroscopic sorption tests, the functions of the above mentioned theoretical models are used. The values of the coefficients obtained in each of the fitted curves are shown in Table 5.

Table 5

Coefficients of the fitted curves for the hygroscopic tests.

Fig. 12. Hygroscopic fitted curves for the LWC type 1.

Fig. 13. Hygroscopic fitted curves for the LWC type 2.

Fig. 14. Hygroscopic fitted curves for the LWC type 3.

Next, the goodness of fit in each of the curves can be observed in Fig. 15:

Fig. 15. The goodness of fit as a function of the coefficient of determination (r^2) for the hygroscopic tests.

From the previous results, it is obtained the following findings:

- The coefficient of determination indicates that the fitted curves to the theoretical models developed for the IEA (Kumaran model) and the MOIST program [31, 32] (Burch model) are the most appropriate to reproduce the hygroscopic

behavior of the tested LWCs. Specifically, the fitted function developed by Burch is a bit better than the Kumaran model.

- The function developed by Kunzel for the WUFI program [27, 28] is the worst-fitting curve and it does not fulfill the requirements of the minimum required goodness.

Therefore, in the hygrothermal fitted curves we will use the Burch model to obtain the moisture content per unit mass as a function of relative humidity for each type of LWC tested.

4.2. Hygrothermal fitted curves and response surface

The conversion of thermal values from a set of conditions (λ_1) to another set of conditions (λ_2) is carried out in accordance with the following expression [19]:

$$\lambda_2 = \lambda_1 \cdot F_T \cdot F_m \cdot F_a \tag{9}$$

In this case, it is assumed that there is no influence of the aging $(F_a = 1)$ and the temperature variation $(F_T = 1)$. The standard rule UNE-EN ISO 10456 [19] establishes a conversion factor, F_{m_i}, for the moisture content as a function of the moisture content per unit mass for the *i*-th set of conditions, u_i, through the conversion coefficient, f_u. In this investigation, we have determined u as a function of the relative humidity using the Burch model as it is indicated in the previous subsection 4.1, giving place to the following equation for the conversion factor [19]:

$$F_{m_i}(\phi) = e^{f_u(u_i(\phi)-u_{50\%})} \tag{10}$$

Until now, Table A.20 in Annex A of the standard rule UNE-EN ISO 10456 [19] takes a conversion coefficient $f_u = 4$ with a moisture content per unit mass ranging from 0 to 0.25 kg/kg, in case of that the expanded clay is used as main aggregate.

Next, Figs. 16, 17 and 18 show the fitted curves corresponding to the thermal conductivity as a function of the relative humidity for the following cases:

1. Value recommended by the standard rule [19] ($f_u = 4$):

$$\lambda(\phi) = \lambda_{50\%} \cdot e^{f_u\left(u_i(\phi)-u_{50\%}\right)} \tag{11}$$

2. Value of conversion coefficient different from the standard rule ($f_u = 16$):

$$\lambda(\phi) = \lambda_{50\%} \cdot e^{f_u\left(u_i(\phi)-u_{50\%}\right)} \tag{12}$$

3. A cubic function :

$$\lambda(\phi) = a \cdot \phi^3 + b \cdot \phi^2 + c \cdot \phi + d \tag{13}$$

where *a*, *b* and *c* are the coefficients of the fitted curve.

4. A logistic function for the conversion coefficient $f_u = 4$ (Logistic plus Standard):

$$\lambda(\phi) = A \cdot \lambda_{50\%} \cdot \frac{1 + m \cdot e^{-\frac{\phi}{B}}}{1 + n \cdot e^{-\frac{\phi}{B}}} \tag{14}$$

where *A* and *B* are the coefficients of the fitted curve.

Fig. 16. Fitted curves corresponding to the thermal conductivity as a function of the relative humidity for the LWC Type 1.

Fig. 17. Fitted curves corresponding to the thermal conductivity as a function of the relative humidity for the LWC Type 2.

Fig. 18. Fitted curves corresponding to the thermal conductivity as a function of the relative humidity for the LWC Type 3.

In this sense, Fig. 19 shows the goodness of fit as a function of the coefficient of determination, r^2, for all the LWC mixes from the laboratory tests. Specifically, the coefficient of determination for the recommended value of the standard rule ranges from 0.28 to 0.33; for the modified value $f_u = 16$, it ranges from 0.66 to 0.83; for the cubic function, it ranges from 0.95 to 0.97; and finally, it ranges from 0.95 to 0.96 for the logistic function.

Fig. 19. The goodness of fit as a function of the coefficient of determination (r^2) for the hygrothermal tests.

The response surface corresponding to the thermal conductivity as a function of the density and the relative humidity for the conversion coefficient $f_u = 4$ [19] corrected by a logistic function is as follows:

$$\lambda(\rho,\phi) = s(\rho)\cdot\lambda_{50\%}(\rho)\cdot F_m(\rho,\phi)\cdot\frac{1+m(\rho)\cdot e^{-\phi/r(\rho)}}{1+n(\rho)\cdot e^{-\phi/r(\rho)}} \quad (15)$$

As might be observed in Fig. 20, the thermal conductivity surface grows if the relative humidity and the material density are increased according to the previous results [7, 11].

Fig. 20. Response surface for specimens made up of the expanded clay (main aggregate) corresponding to the fitted curve according to the Standard $(f_u = 4)$ [19], amended by a logistic function.

Table 6 shows the specific values of the LWC thermal conductivity as a function of the most representative values of the density with respect to the relative humidity within the range studied.

Table 6

Values of the LWC thermal conductivity as a function of the most representative values of the density with respect to the relative humidity.

5. Conclusions

Based on the experimental results and numerical fitting study of this investigation, the following findings can be drawn:

1. A new experimental procedure for the calculation of the hygroscopic sorption isotherm curves based on the standard UNE-EN ISO 12571:2000 [22] was

developed, and it was applied to the study of the hygroscopic properties of three different LWC mixes with success.

2. We have compared the experimental results with the theoretical models developed by Kumaran, Burch and Kunzel [27-32] and we have calculated the best fitting parameters in each one of them. As a consequence, it is shown that the Burch model is the most suitable to reproduce the actual hygroscopic behavior of the LWCs tested.
3. A new testing methodology was built to obtain the hygrothermal properties based on the standards UNE-EN ISO 8990 and ASTM C 1363 [20, 21], and it was applied to the study of the hygrothermal behaviour of three different LWC mixes.
4. From the hygrothermal tests, the best-fitting curves based on analytical functions and the standard rule UNE-EN ISO 10456 [19] have been obtained. It is possible to state that the values of the conversion coefficients used in the standard rule in case of expanded clay as the main aggregate of the LWC material must be updated according to our laboratory tests.

Finally, this research work proposes for all the LWC mixes, with densities between 900 and 1400 kg/m^3 and moisture content ranging from 0 to 0.25 kg/kg, a change of the standard rule's conversion coefficients from 4 to 16 (see Table A.20. of the standard [19]). Other two feasible possibilities are:

- A logistic function with a conversion coefficient $f_u = 4$. This fitted curve shows a hygrothermal behavior in agreement with the laboratory tests.

- A cubic function also presents a good fit from the hygrothermal point of view according to the laboratory tests.

Acknowledgements

The authors wish to acknowledge the partial financial support provided by Spanish Ministry of Science and Innovation through the Research Projects BIA2008-00058, BIA2012-31609, and the support provided by the Research Project FICYT PC-10-33 and the Gijon City Council research fellowship SV-12-GIJON-1. We also thank the GICONSIME Research Group, the Department of Construction at University of Oviedo and the WEBER-MAXIT Group. English grammar and spelling of this manuscript have been revised by a native person.

References

[1] Carmeliet J, Roels S. Determination of the moisture capacity of porous building materials. J Building Phys 2002; 25: 209-237.

[2] Bouchair A. Steady state theoretical model of fired clay hollow bricks for enhanced external wall thermal insulation. Build Environ 2008; 43(10): 1603-1618.

[3] Sandberg I. Effects of moisture on the thermal performance of insulating materials, Moisture control in Buildings: the key factor in mold prevention. 2nd ed. New York: H.R. Trechsel and M.T. Bomberg; 2009.

[4] Shannag MJ. Characteristics of lightweight concrete containing mineral admixtures. Constr Build Mater 2011; 25: 658-662.

[5] Li LP, Wu ZG, He YL, Lauriat G, Tao WQ. Optimization of the configuration of 290×140×90 hollow clay bricks with 3-D numerical simulation by finite volume method. Energy Build 2008; 40(10): 1790-1798.

[6] Cui HZ, Yiu Lo T, Ali Memon S, Xu W. Effect of lightweight aggregates on the mechanical properties and brittleness of lightweight aggregate concrete. Constr Build Mater 2012; 35:149-158.

[7] del Coz Diaz JJ, Garcia Nieto PJ, Dominguez Hernandez J, Suarez Sanchez A. Thermal design optimization of lightweight concrete blocks for internal one-way spanning slabs floors by FEM. Energy Build 2009; 41(12): 1276-1287.

[8] Yasar E, Erdogan Y. Strength and thermal conductivity in lightweight building materials. Bull Eng Geol Environ 2008; 67(4): 513-519.

[9] Othuman MA, Wang YC. Elevated-temperature thermal properties of lightweight foamed concrete. Constr Build Mater 2011; 25(2): 705-716.

[10] Al-Sibahy A, Edwards R. Thermal behaviour of novel lightweight concrete at ambient and elevated temperatures: Experimental, modelling and parametric studies. Constr Build Mater 2012; 31: 174-187.

[11] Gawin D, Kosny J, Desjarlais A. Effect of moisture on thermal performance and energy efficiency of buildings with lightweight concrete walls. In: Proceedings ACEEE Summer Study on Energy Efficiency in Buildings 2000, Vol. 3, pp. 3149-3160.

[12] Qin M, Aït-Mokhtar A, Belarbi R. Two-dimensional hygrothermal transfer in porous building materials. Appl Therm Eng 2010; 30(16): 2555-2562.

[13] Lu X. Modelling of heat and moisture transfer in buildings I. Model Program, Energy Build 2002; 34: 1033–1043.

[14] Talukdar P, Olutmayin SO, Osanyintola OF, Simonson CJ. An experimental data set for benchmarking 1-D, transient heat and moisture transfer models of hygroscopic building materials. Part I: Experimental facility and material property data. Int J Heat Mass Transfer 2007; 50(23-24): 4527-4539.

[15] Kreith F, Bohn MS. Principles of heat transfer. New York: Thomson-Engineering; 2000.

[16] Abahri K, Belarbi R, Trabelsi A. Contribution to analytical and numerical study of combined heat and moisture transfers in porous building materials. Build Environ 2011; 46(7): 1354-1360.

[17] del Coz Díaz JJ, Lozano Martínez-Luengas A, Adam JM, Rodríguez AM. Non-linear hygrothermal failure analysis of an external clay brick wall by FEM - A case study. Constr Build Mater 2011; 25(12): 4454-4464.

[18] dos Santos GH, Mendes N. Heat, air and moisture transfer through hollow porous blocks. Int J Heat Mass Transfer 2009; 52(9-10): 2390-2398.

[19] UNE-EN ISO 10456:1999 (ISO 10456:1999). Building materials and products. Procedures for determining declared and design thermal values.

[20] ASTM C 1363 – 97. Standard test method for the thermal performance of building assemblies by means of a Hot Box apparatus.

[21] UNE-EN ISO 8990:1997. Thermal insulation. Determination of steady-state thermal transmission properties. Calibrated and guarded hot-box (ISO 8990:1994).

[22] ISO 12571:2000 Standard. Hygrothermal performance of building materials and products. Determination of hygroscopic sorption properties.

[23] UNE-EN ISO 7345:1996 (ISO 7345:1987). Thermal insulation. Physical quantities

[24] Fox J. Applied regression analysis and generalized linear models. London: Sage Publications; 2008.

[25] Dunesche P, Remillard B. Statistical modeling and analysis for complex data problems. New York: Springer; 2010.

[26] Chapman SJ. Essentials of MATLAB programming. Stamford (USA): CL-Engineering; 2008.

[27] Künzel HM. Simultaneous heat and moisture transport in building components, one- and two-dimensional calculation using simple parameters. Stuttgart (Germany): Ph.D. Dissertation, IRB-Verlag Fraunhofer-Institut für Bauphysik; 1995.

[28] Krus M. Moisture transport and storage coefficients of porous mineral building materials. Theoretical principles and new test methods. Stuttgart (Germany): Internal Report, Fraunhofer IRB Verlag; 1996.

[29] Kumaran KM. Heat, air and moisture transport in envelope parts. Final report. Task 3 material properties. Leuven: Internal report, IEA. ECBCS; 1996.

[30] Kumaran KM. Moisture control in buildings. In: ASTM Manual Series, Heinz R. Trechsel editorial series; 1994.

[31] Burch DM, Thomas WC, Fanney AH. Water vapor permeability measurements of common building materials. In: ASHRAE Transactions, No. 98, Vol. 2; 1992.

[32] Burch DM, Chi J. MOIST. A PC program for predicting heat and moisture transfer in building envelopes. In: NIST Special Publication 917, Gaithersburg. MD: National Institute of Standards and Technology; 1997.

LIST OF TABLES:

Table 1

Mix proportions of the LWC samples.

Composition SAMPLE	LWA(*) (kg)	LWS(*) (kg)	Silica sand (kg)	Cement (kg)	Water (kg)
1A	0.84	0.72	0.48	0.495	0.36
1B	0.84	0.72	0.48	0.495	0.36
2A	0.78	0.72	0.675	0.54	0.36
2B	0.78	0.72	0.675	0.54	0.36
3A	0.84	0	2.4	0.54	0.39
3B	0.84	0	2.4	0.54	0.39

(*)Note: LWA: 4-12.5 mm particle diameter, and LWS: 1-5 mm particle diameter.

Table 2

Densities of the LWC determined in this investigation during the manufacturing process.

Sample	Fresh density (kg/m^3)	Oven dry density (kg/m^3)	Equilibrium density (kg/m^3)
1A	1027	953	973
1B	992	948	971
2A	1055	979	999
2B	1058	1,001	1,026
3A	1460	1,353	1,373
3B	1460	1,338	1,362

Table 3

Experimental results of the LWC moisture content per unit mass (kg/kg) for the relative humidity (%) points tested.

	ϕ (%)									
LWC type	**10**	**15**	**22**	**35**	**50**	**65**	**75**	**80**	**85**	**95**
1	0.0111	0.0134	0.0150	0.0165	0.0179	0.0194	0.0209	0.0225	0.0238	0.0251
2	0.0102	0.0127	0.0147	0.0161	0.0176	0.0195	0.0209	0.0224	0.0237	0.0250
3	0.0069	0.0086	0.0099	0.0110	0.0119	0.0131	0.0138	0.0148	0.0158	0.0166

Table 4

Experimental results of the LWC thermal properties for a relative humidity equal to 50%.

Sample	*Density* (Kg/m^3)	q (W/m^2)	ΔT (K)	U (W/m^2K)	R (m^2K/W)	λ (W/mK)	ϕ (%)
1A	973	96.357	19.647	4.904	0.284	0.176	50
1B	971	95.839	20.058	4.778	0.289	0.173	50
2A	999	93.319	17.598	5.303	0.269	0.186	50
2B	1,026	94.533	17.549	5.387	0.266	0.188	50
3A	1,373	115.260	13.075	8.815	0.193	0.258	50
3B	1,362	114.068	13.142	8.680	0.195	0.256	50

Table 5

Coefficients of the fitted curves for the hygroscopic tests.

	Kunzel model (WUFI)		Kumaran model (IEA)		Burch model (MOIST)
LWC type 1					
w_{lim}	23.9438	*a*	– 0.04039605	*A*	17.6040545
b	– 0.22	*b*	0.0743672	*B*	0.16239767
		c	0.00134979		
LWC type 2					
w_{lim}	24.8773	*a*	– 0.03632732	*A*	17.9412727
b	– 0.25	*b*	0.06867017	*B*	0.16754437
		c	0.00222107		
LWC type 3					
w_{lim}	21.8496	*a*	– 0.03991617	*A*	15.9342307
b	– 0.23	*b*	0.0769837	*B*	0.16351604
		c	0.0023988		

Table 6

Values of the LWC thermal conductivity as a function of the most representative values of the density with respect to the relative humidity.

Standard + Logistic	ρ **(kg/m^3)**										
ϕ ***(%)***	900	950	1,000	1,050	1,100	1,150	1,200	1,250	1,300	1,350	1,400
0	0.136	0.154	0.171	0.185	0.199	0.211	0.221	0.230	0.237	0.243	0.247
5	0.137	0.155	0.171	0.186	0.199	0.211	0.222	0.231	0.238	0.244	0.248
10	0.137	0.155	0.172	0.187	0.200	0.212	0.223	0.231	0.239	0.244	0.249
15	0.138	0.156	0.172	0.187	0.201	0.213	0.223	0.232	0.240	0.245	0.250
20	0.138	0.156	0.173	0.188	0.202	0.214	0.224	0.233	0.241	0.246	0.251
25	0.139	0.157	0.174	0.189	0.203	0.215	0.225	0.234	0.242	0.247	0.252
30	0.140	0.158	0.175	0.190	0.204	0.216	0.227	0.236	0.243	0.249	0.253
35	0.140	0.159	0.176	0.191	0.205	0.217	0.228	0.237	0.244	0.250	0.254
40	0.142	0.160	0.177	0.193	0.207	0.219	0.230	0.239	0.246	0.252	0.256
45	0.143	0.162	0.179	0.195	0.209	0.221	0.232	0.241	0.248	0.254	0.258
50	0.145	0.164	0.181	0.197	0.211	0.224	0.234	0.243	0.251	0.256	0.260
55	0.147	0.167	0.184	0.200	0.215	0.227	0.238	0.247	0.254	0.260	0.264
60	0.150	0.170	0.188	0.205	0.219	0.232	0.243	0.251	0.259	0.264	0.268
65	0.155	0.176	0.194	0.211	0.226	0.238	0.249	0.258	0.265	0.270	0.273
70	0.161	0.183	0.202	0.219	0.234	0.247	0.258	0.267	0.273	0.278	0.281
75	0.170	0.193	0.213	0.231	0.247	0.260	0.270	0.278	0.285	0.289	0.291
80	0.182	0.207	0.228	0.247	0.263	0.276	0.287	0.295	0.300	0.303	0.304
85	0.198	0.224	0.248	0.268	0.285	0.298	0.309	0.316	0.321	0.322	0.322
90	0.217	0.246	0.272	0.294	0.312	0.326	0.336	0.343	0.347	0.347	0.345
95	0.240	0.272	0.299	0.323	0.343	0.358	0.369	0.376	0.379	0.378	0.374
100	0.263	0.298	0.329	0.355	0.377	0.394	0.406	0.413	0.415	0.414	0.408

Figure

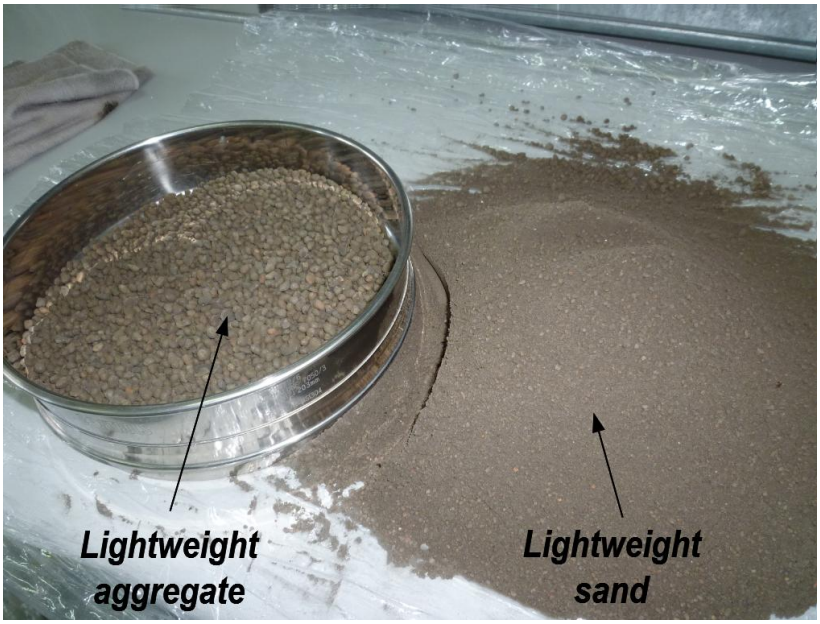

Fig. 1. Expanded clay aggregates used in this research: LWA (left) and LWS (right).

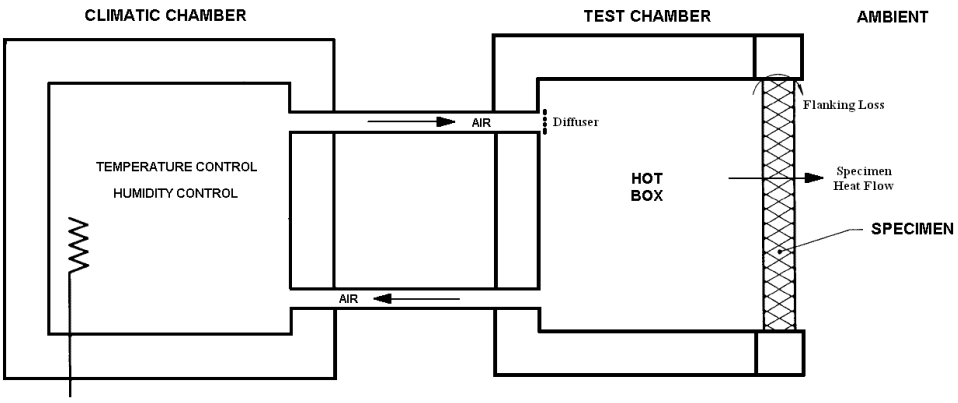

Fig. 2. Scheme of the experimental facility layout.

Fig. 3. Photographs of the climatic chamber (left) and hot-box apparatus (right).

Fig. 4. Experimental setup (left) and specimens located inside the hot-box test chamber (right) for hygroscopic tests.

(a) **(b)** **(c)**

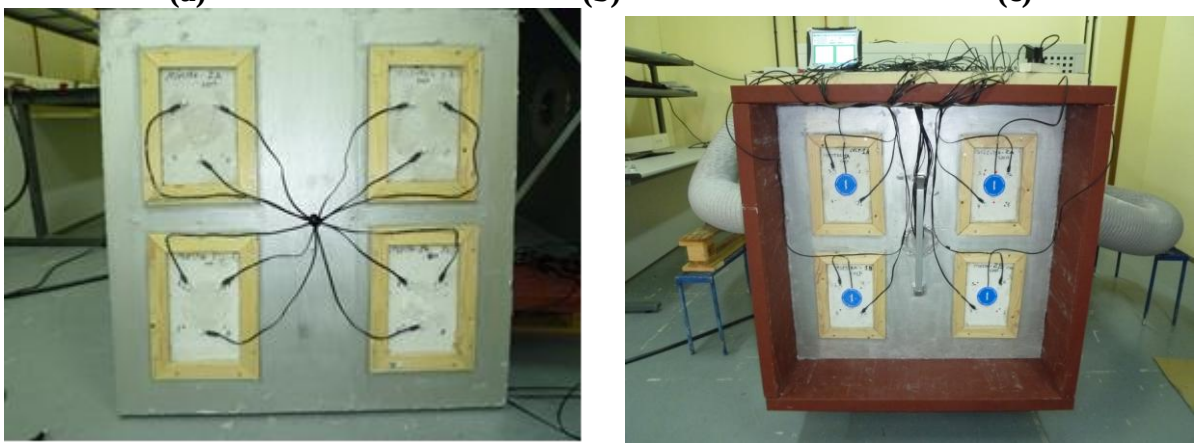

(d) **(e)**

Fig. 5. Hygrothermal test setup: (a) a filter cap type SF1, (b) a hygrothermal sensor type SHT75, (c) a thermal flux sensor type HP01, (d) specimens with hygrothermal sensors located on the inner side, (e) specimens with hygrothermal and thermal flux sensors on the external side.

Fig. 6. Data acquisition system from temperature and humidity sensors type SHT75.

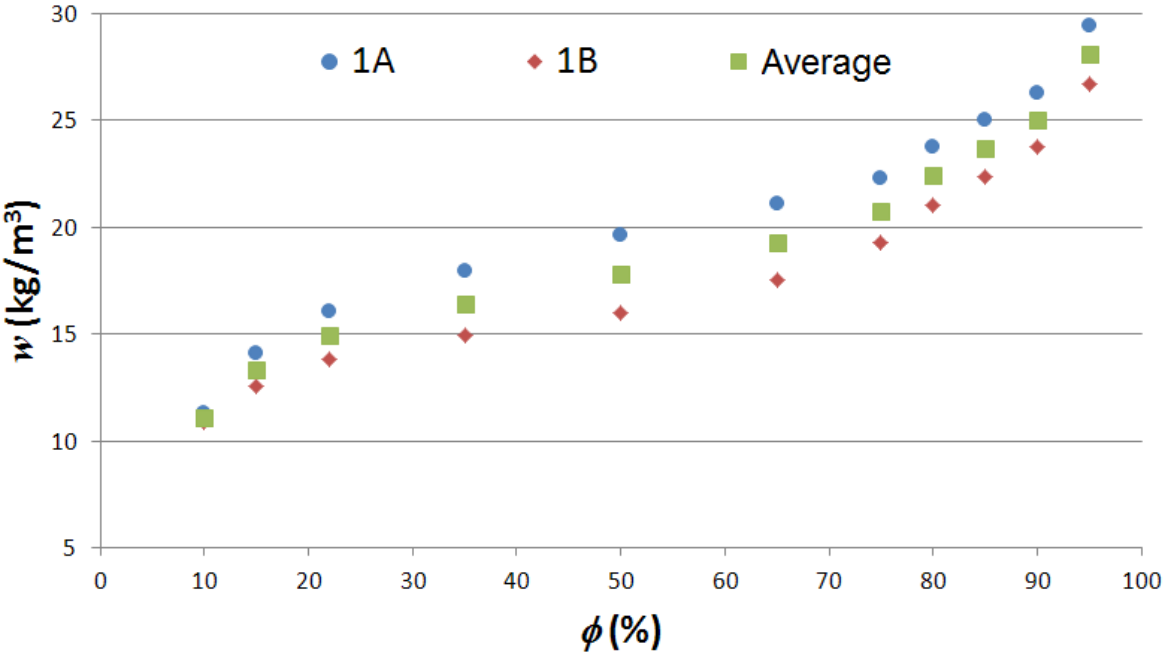

Fig. 7. Sorption isotherms of the LWC samples type 1.

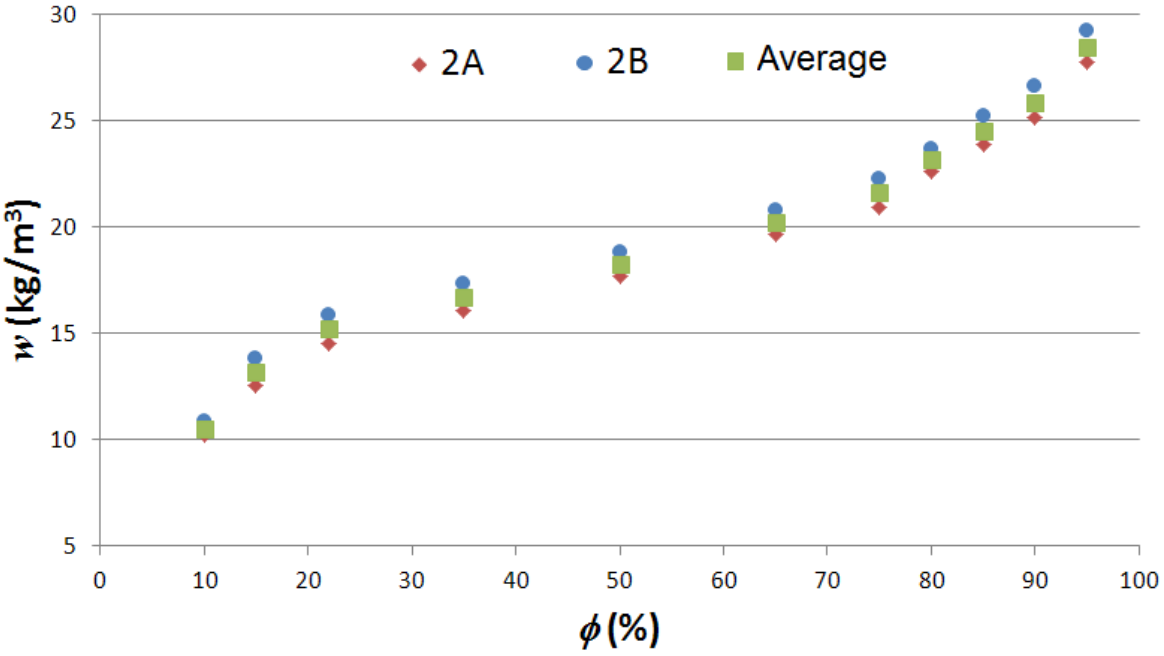

Fig. 8. Sorption isotherms of the LWC samples type 2.

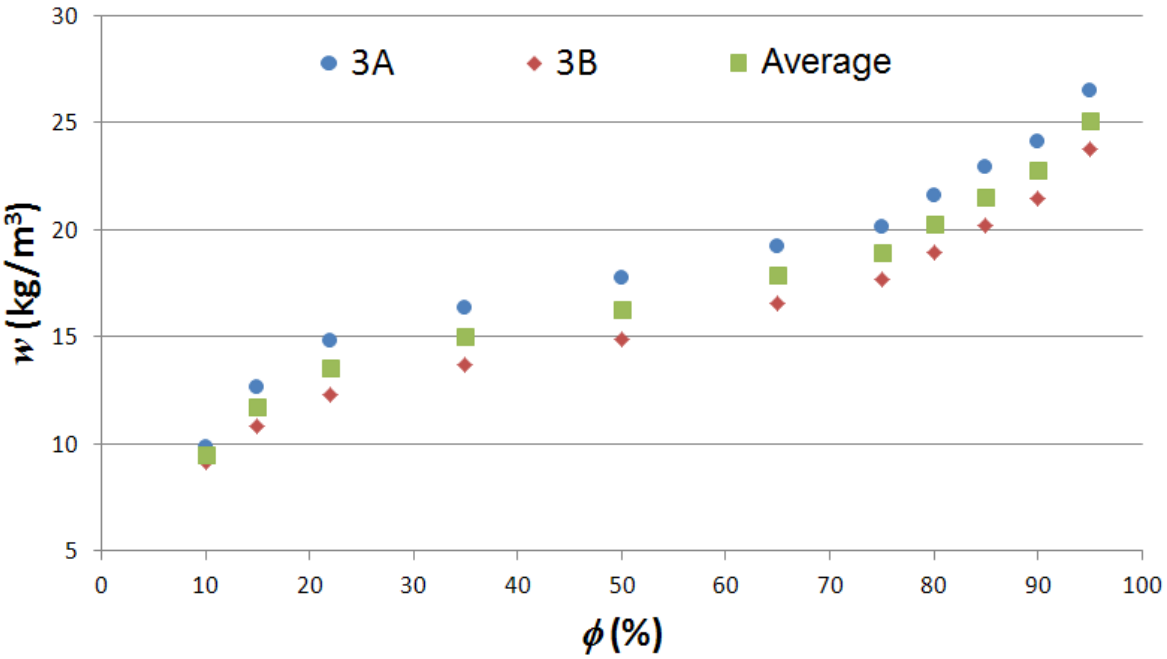

Fig. 9. Sorption isotherms of the LWC samples type 3.

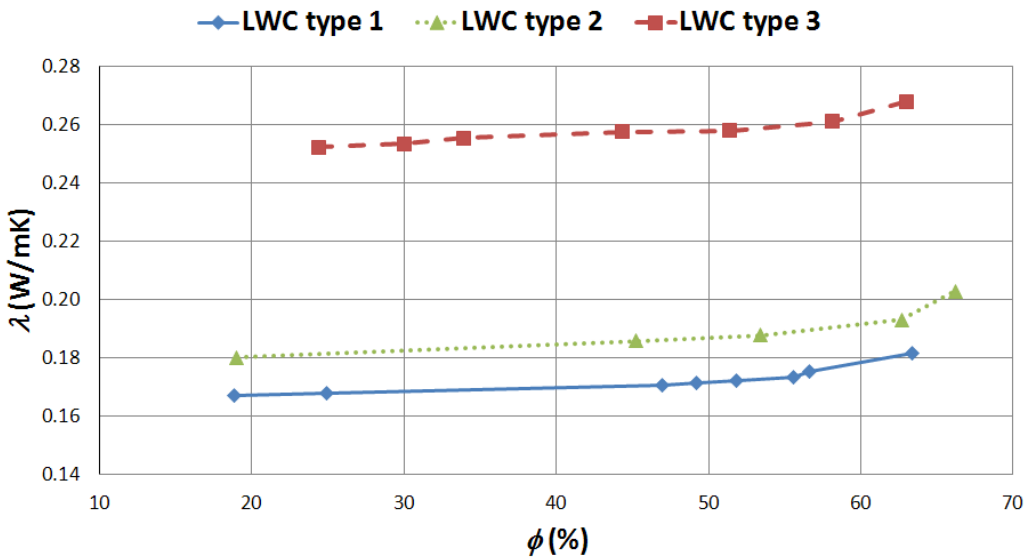

Fig. 10. Thermal conductivity (λ) versus relative humidity (ϕ) curves for the three different mixtures of LWC.

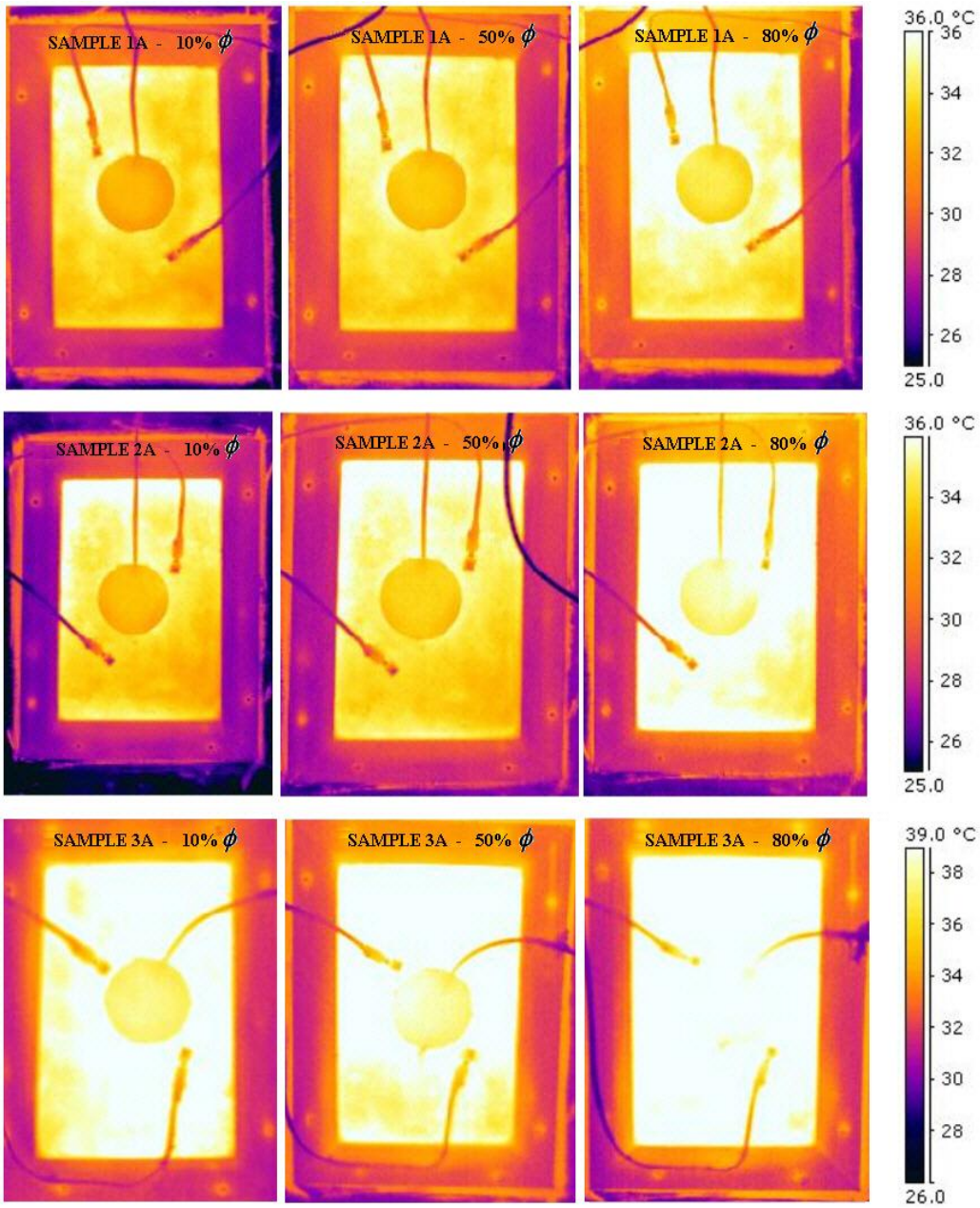

Fig. 11. Thermal photographs of three samples for different relative humidities: 10% (left), 50% (middle) and 80% (right).

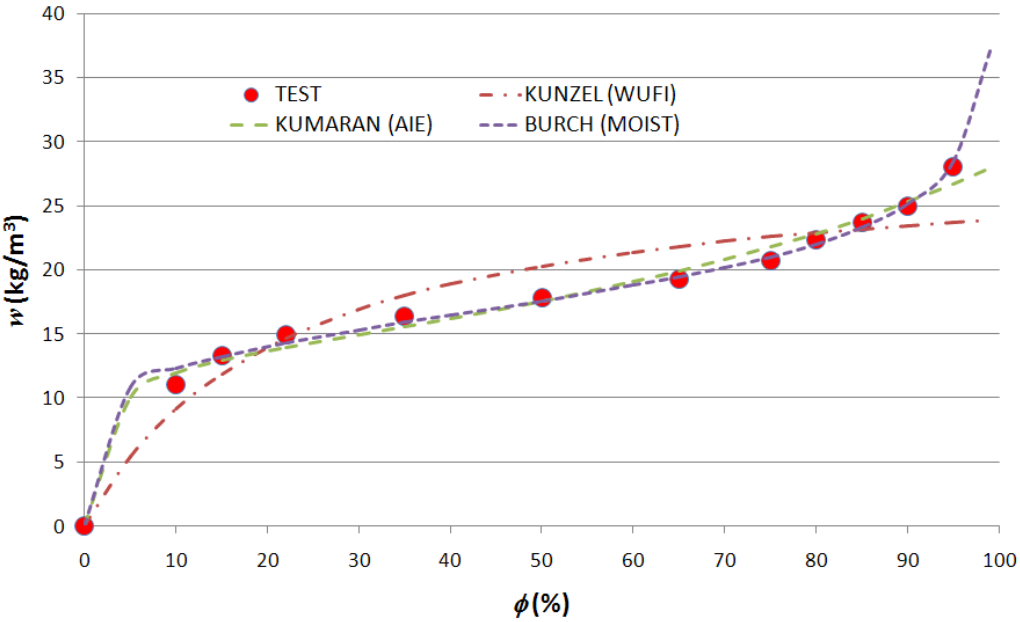

Fig. 12. Hygroscopic fitted curves for the LWC type 1.

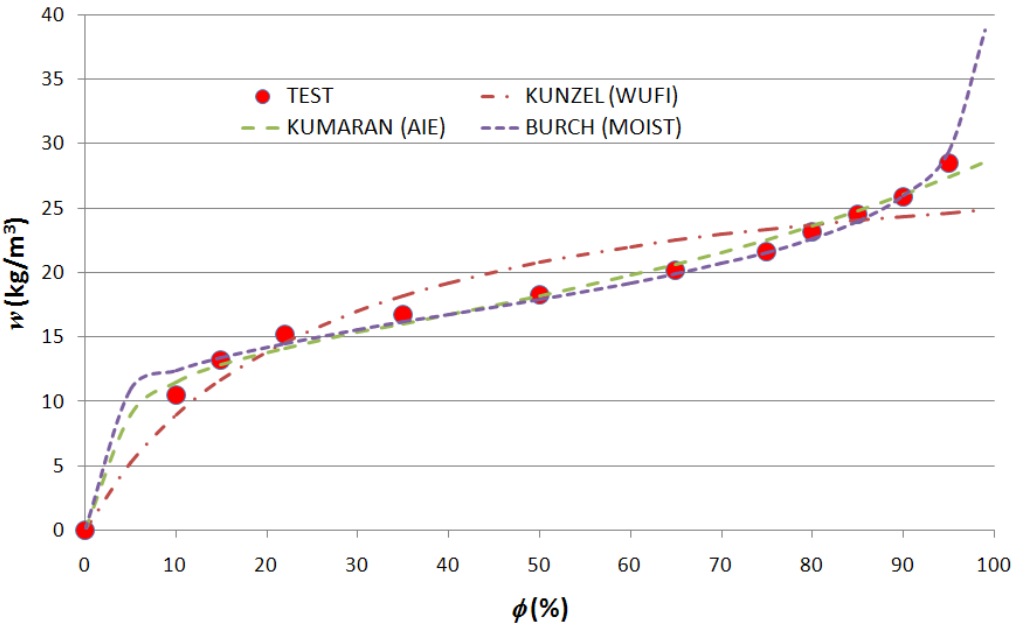

Fig. 13. Hygroscopic fitted curves for the LWC type 2.

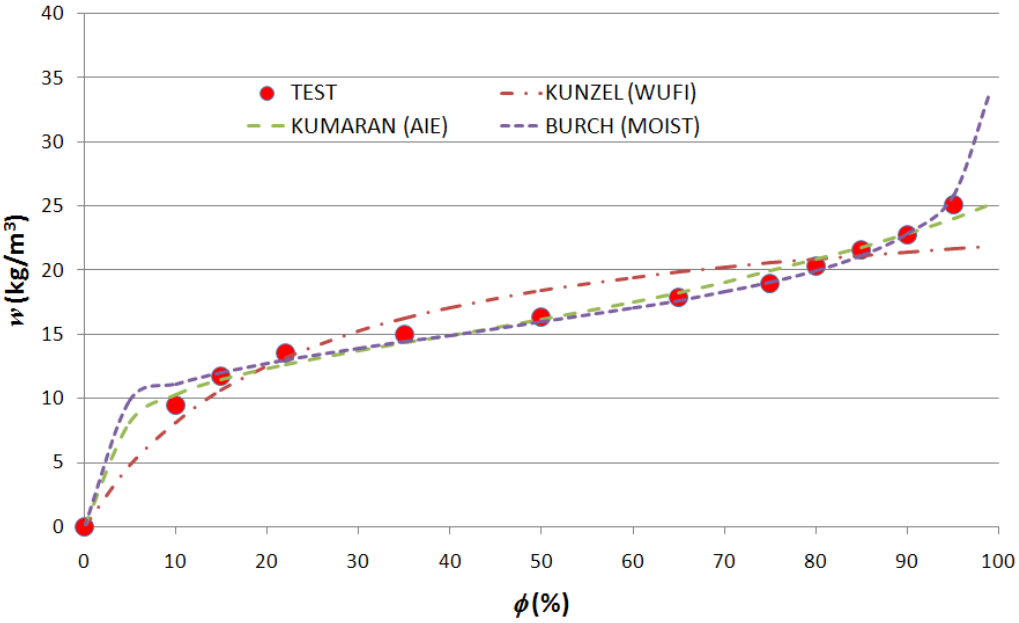

Fig. 14. Hygroscopic fitted curves for the LWC type 3.

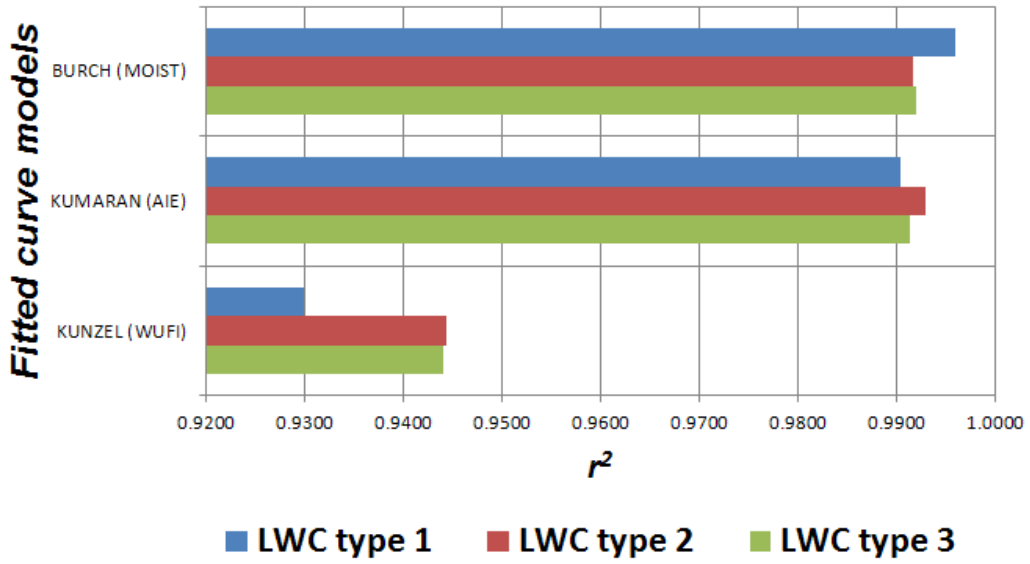

Fig. 15. The goodness of fit as a function of the coefficient of determination (r^2) for the hygroscopic tests.

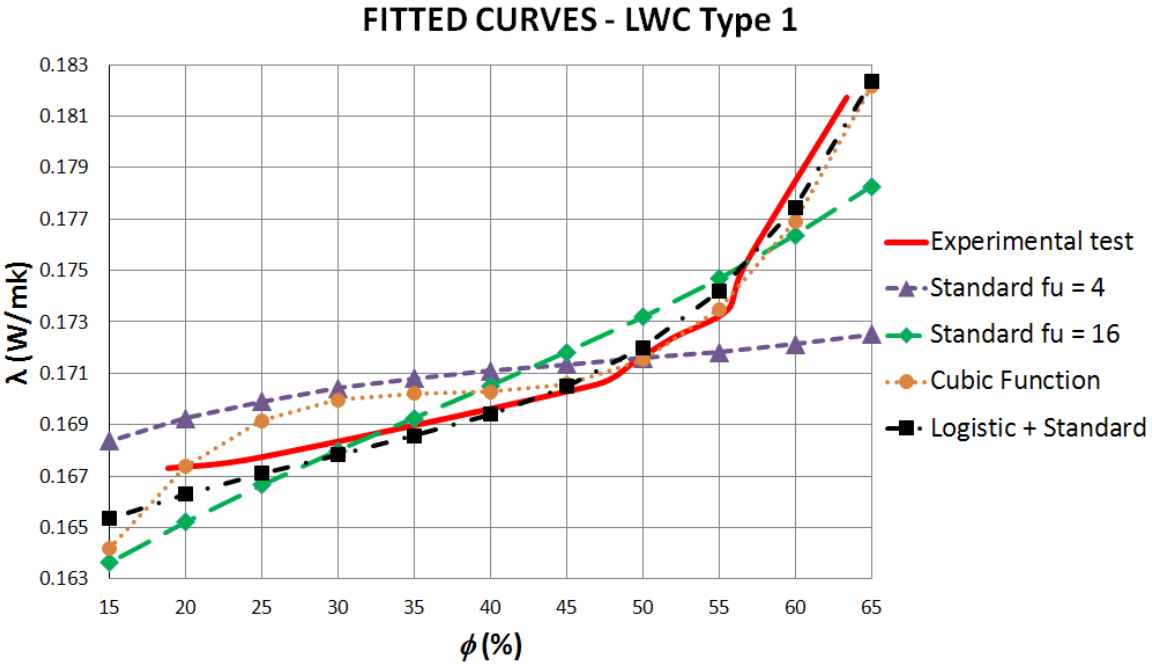

Fig. 16. Fitted curves corresponding to the thermal conductivity as a function of the relative humidity for the LWC Type 1.

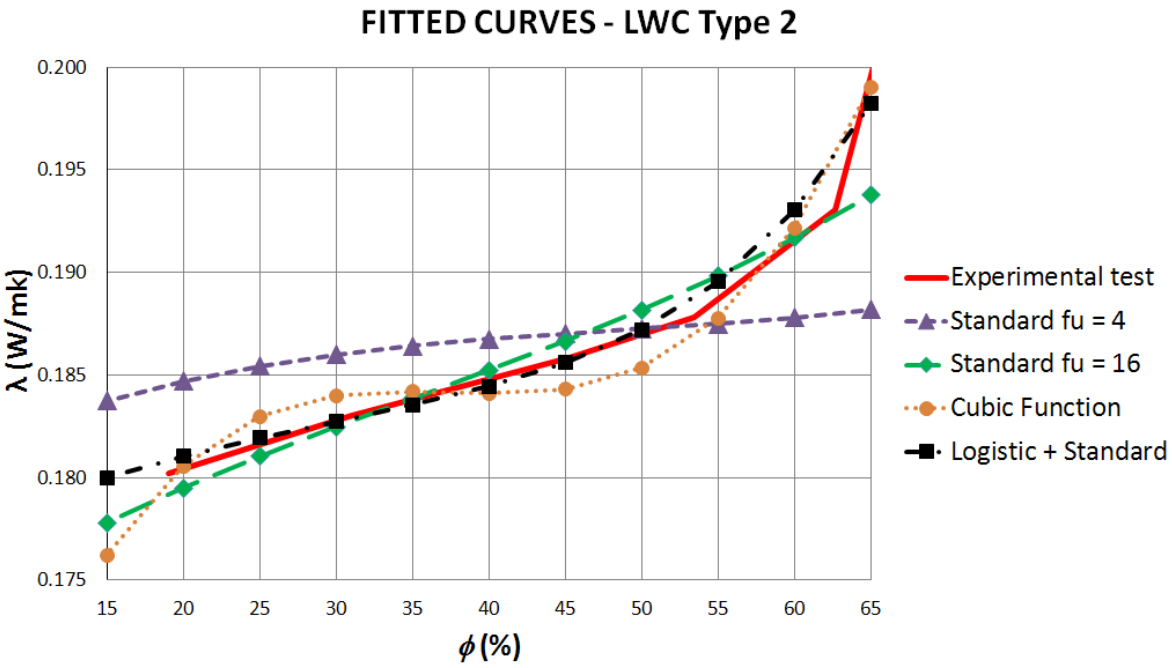

Fig. 17. Fitted curves corresponding to the thermal conductivity as a function of the relative humidity for the LWC Type 2.

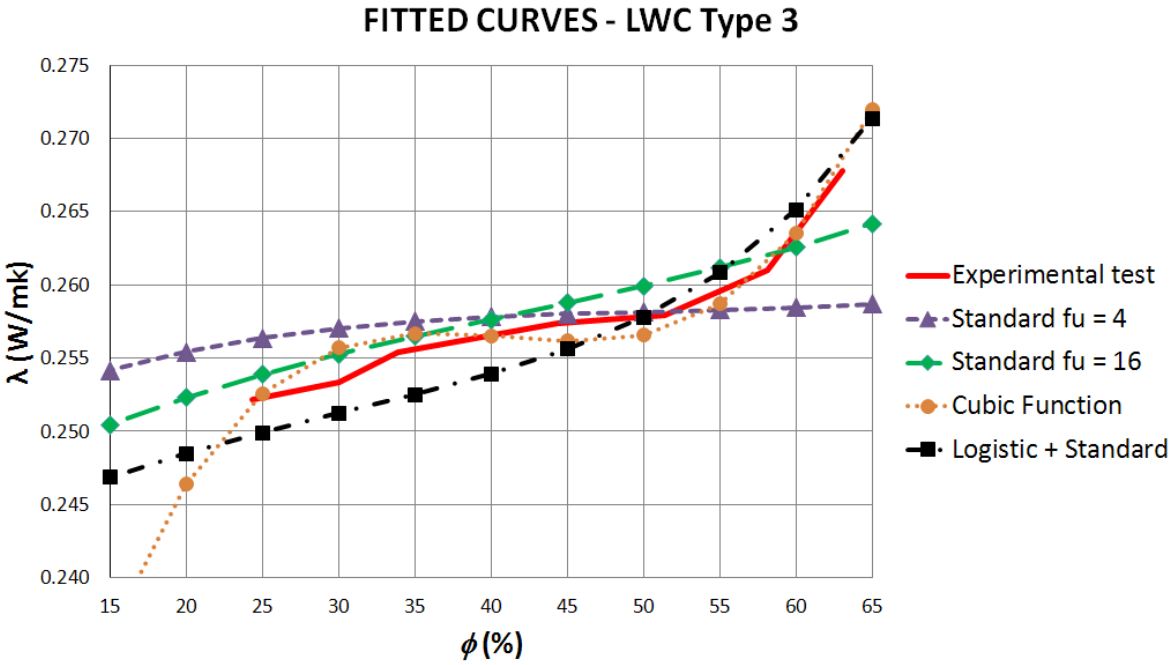

Fig. 18. Fitted curves corresponding to the thermal conductivity as a function of the relative humidity for the LWC Type 3.

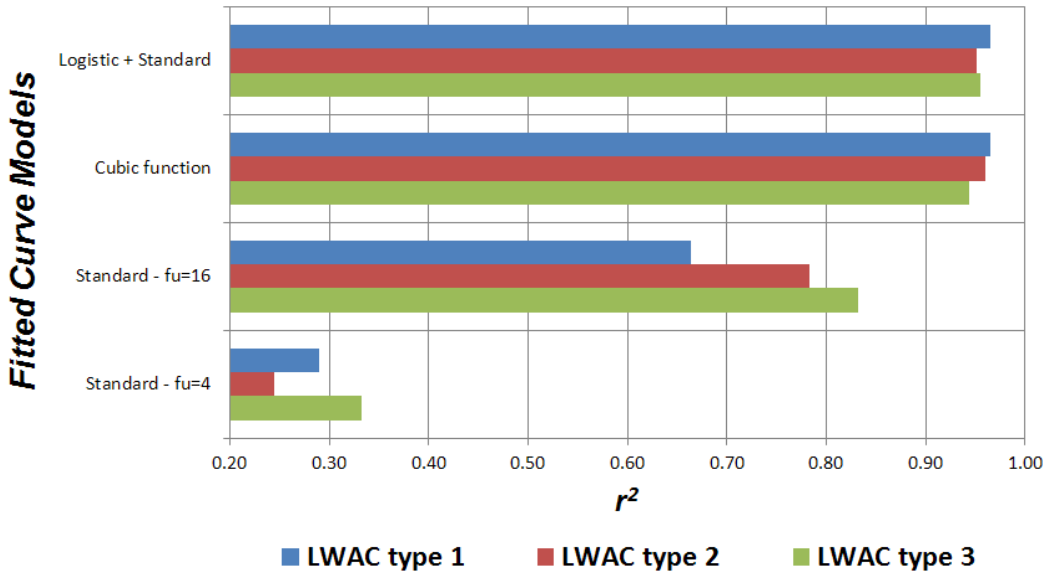

Fig. 19. The goodness of fit as a function of the coefficient of determination (r^2) for the hygrothermal tests.

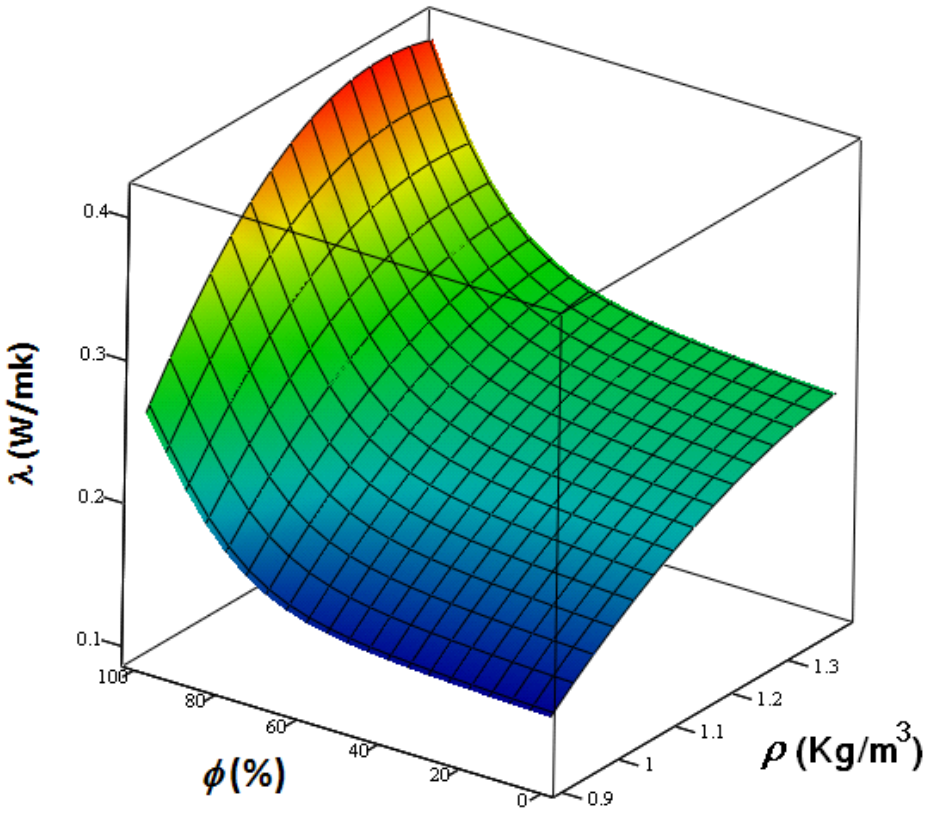

Fig. 20. Response surface for specimens made up of the expanded clay (main aggregate) corresponding to the fitted curve according to the Standard $(f_u = 4)$ [19], amended by a logistic function.